Applied Surface Science 31 (1988) 59–71
North-Holland, Amsterdam

REVIEW

ADVANCES IN MICROSCOPY: SCANNING TUNNELING AND ELECTRON POLARIZATION MICROSCOPY *

Robert J. CELOTTA

National Bureau of Standards, Gaithersburg, MD 20899, USA

Received 29 September 1986; accepted for publication 22 November 1986

An overview is presented of two new techniques that can be used to study the physical, electronic, and/or magnetic microstructure of surfaces. The method of scanning tunneling microscopy has emerged as a powerful way of observing physical structure down to the atomic level and is being extended to give further insight into surface electronic structure over atomic dimensions as well. Scanning electron microscopy with polarization analysis is being applied to the study of magnetic microstructures with sizes down to 10 nm and is capable of demonstrating the effect that physical microstructure has on magnetic domains. Discussions of both techniques will include descriptions of the method, the apparatus used and some examples of current applications.

1. Introduction

Research on microstructures is receiving greater attention in many different areas. From a practical point of view new devices based on microfabrication may offer decreased cost and higher performance. From a scientific point of view, many very interesting questions are raised when "size effects" become important, that is when a large fraction of the atoms lie near an interface. From a technological point of view, such size effects can be used to produce new devices or materials with specially tailored properties. Two new measurement methods, scanning tunneling microscopy and scanning electron microscopy with polarization analysis, have recently emerged and now allow a direct observation of physical and magnetic microstructure and a determination of their effect on the electronic or magnetic properties of material.

This paper will present an overview of these rapidly changing new areas of research. The intention is to provide a description of the basic method, instrumentation, and illustration of some of the applications. The interested

* This article was one of a series of invited review papers presented at the ASTM symposium on "Recent Developments in Surface Spectroscopy/Analysis", held as part of the 1986 Pittsburgh Conference on Analytical Chemistry and Applied Spectroscopy, which took place in Atlantic City, New Jersey on 12 March 1986.

0169-4332/88/$03.50

reader will find more details in the extensive list of publications provided in the references [1].

2. Scanning tunneling microscopy

A traditional method of observing surface microtopography involves the use of a diamond stylus scanned across a sample surface [2]. In 1972, Young devised a non-contacting technique [3–5] based on scanning a field emitter across a conducting surface and making use of the rapid variation in field emission current with distance to maintain a constant tip-to-surface distance with the help of piezoelectric transducers and a feedback system. With this device, surface regions with dimensions of up to a few microns were mapped with a sub-atomic vertical resolution and a lateral resolution of 400 nm. Later, in a similar but non-scanning device, the tip was moved sufficiently close to the surface so that the emission process corresponded to metal–vacuum–metal tunneling [5,6]. It was not until 1982 that Binnig and Rohrer [7] demonstrated the spectacular result that with an apparatus capable of scanning while in the vacuum tunneling regime it was possible to image individual atoms in the 7×7 reconstruction of the Si(111) surface as shown in fig. 1. This landmark paper stimulated the rapid growth [1] of the field of scanning tunneling microscopy. In 1986 Binnig and Rohrer were awarded the Nobel Prize in Physics for their design of the scanning tunneling microscope (STM).

2.1. Method

The physical basis of the operation of an STM involves measurement of the tunneling current present across a vacuum gap when two conducting electrodes at different potentials are spaced a few ångströms apart. Electrons from the negative electrode tunnel through a potential barrier into unfilled states of the positive electrode. This effect can be modeled by using the transfer Hamiltonian theory developed by Bardeen [8] in which the current is proportional to the overlap between the wave function of the filled state in which the electron originates and that of its empty state destination. An example of a quantitative application of this theory has been given by Tersoff and Hamann [9,10] for the Au(110) surface. An approximate representation for the current J in the gap is, for the case of small bias voltages,

$$J \propto V \mathrm{e}^{-(A\phi_0^{1/2}d)},$$

where V is the voltage difference across the gap, ϕ_0 is the barrier height, sometimes called the average work function, and d is the distance between the tip and the surface. If d is measured in ångströms and ϕ_0 in electron volts, the constant A has a value of approximately 1.025 $(\mathrm{eV})^{-1/2}\,\mathrm{Å}^{-1}$. Therefore, for a

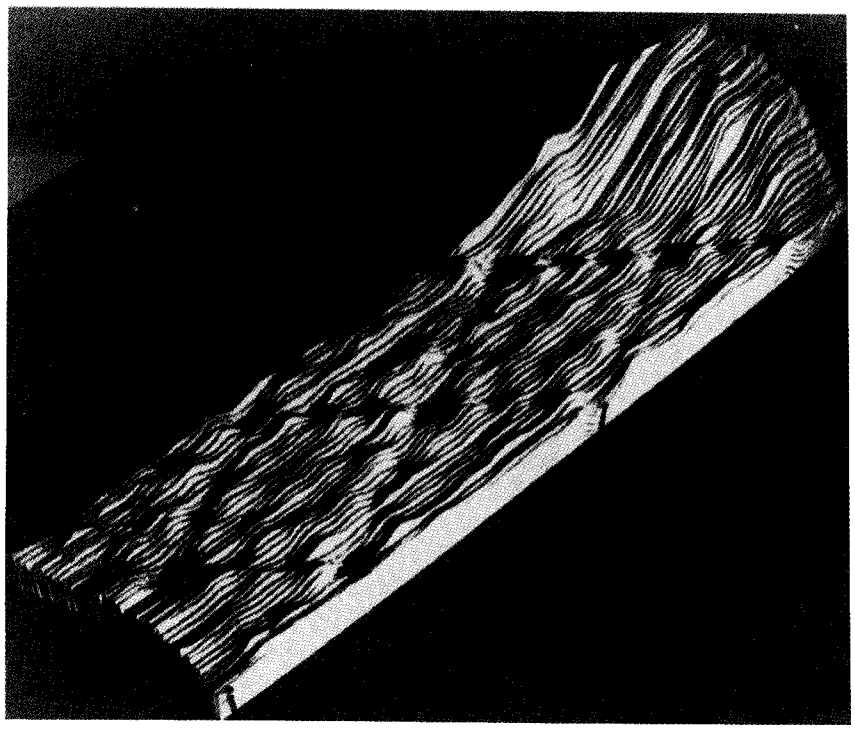

Fig. 1. Relief map of the 7×7 reconstruction of the Si(111) surface showing two complete unit cells. Taken from ref. [7].

typical barrier height of a few eV, the current density will change by an order of magnitude for a change in the gap distance of 1 Å. If the STM is operated in a constant voltage mode then the tunneling current observed varies exponentially with the gap distance, thereby providing a very sensitive measure of the gap spacing on the atomic scale.

In a typical embodiment of a scanning tunneling microscope [11] a flat conducting surface is positioned opposite a pointed metal tip as shown schematically in fig. 2. The tip is mounted to three orthogonal piezoelectric elements capable of making smooth displacements of atomic dimensions with the application of convenient voltages, e.g. a few nanometers per volt applied. The constant gap voltage applied, typically 10 meV for metal electrodes, produces a tunneling current of approximately 1 nA which is controlled by a feedback system. The servo system maintains a constant gap distance by applying a suitable voltage to the normal (z-axis) piezo-electric element to keep the tunneling current at a preset constant value. Measurement of the piezo-electric voltage required as a function of time provides a direct measure

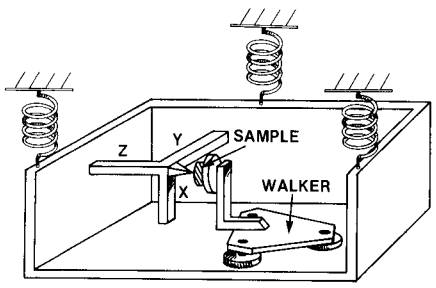

Fig. 2. Schematic representation of a typical scanning tunneling microscope. Rectangular members labeled X, Y and Z are three orthogonal piezoelectric tip positioners.

of changes in the gap distance which required servo correction. The other two piezo drives are used to raster scan the tip across an area of the surface. The feedback mechanism will constantly adjust the tip position to maintain a constant gap distance and will follow the surface contour at a distance of a few ångströms. If a cathode ray tube is scanned in synchronism with the tip and the intensity displayed at each point is proportional to the *z*-axis piezo voltage, then a "gray scale" image of the surface topography can be obtained. The design and construction of a UHV compatible STM have been described by van de Walle et al. [12].

Given the basic idea for this new type of microscope, a number of significant questions immediately arise. First, to observe topographic modulations of atomic order the gap distance modulations caused by ambient vibrations must be extremely small. One method of vibration isolation is illustrated schematically in fig. 2. A frequently used technique [11] involves the use of two stages of spring suspension. Such systems, unfortunately, isolate much better at higher frequencies than at lower frequencies. This emphasizes the need to make the sample–tip support structure as rigid as possible, since this places the lowest normal mode at a high frequency which can effectively be attenuated by the spring suspension system. Some of the more recent designs [13] make use of a set of stacked plates with elastomer spacers as a vibration damper. Additional attempts to make the tip–sample assembly very rigid have proven successful [14].

Since the motion of the *z*-axis piezo has a relatively limited range, a system of positioning the sample within this scan range is required. Some systems make use a "walker" device (fig. 2) which again uses piezo electric transducers to make micro-sized displacements. The end points of the piezo electric device can alternately be held down or released from the supporting table by electrostatic forces. With a series of "crab-like" steps, and with optical observation, these devices can position the sample within the servo system range.

The lateral resolution of the STM depends on both the gap distance and the effective size of the tip [9,10]. Since atomic resolution has been observed in a number of systems it is argued that the effective tunneling site on the tip must be limited to one atom or, at most, a few atoms at the tip. Since the fabrication procedures for tips at present are not thought to produce perfectly shaped needles down to the active site, it follows that only the atom closest to the surface is active because of the rapid decrease of tunneling current with gap distance. While this model justifies the measurement of flat, single crystal surfaces with tips of unknown profile, any substantial surface corrugation increases the measurement uncertainty since other parts of the tip may become active tunneling sites if they pass nearer to the surface during a scan.

2.2. Applications of the STM

The use of the STM is expanding very rapidly, in both the number and variety of applications. Studies of surface reconstruction have played a large role in establishing the usefulness of the technique. In addition to the initial work of Binnig and Rohrer shown in fig. 1, there have been additional studies of the Si(111)-7×7 surface [15–17]. They include the observation of surface states [15], and the imaging of single atom high steps [16] in registry with the pattern of the 7×7 reconstruction. Feenstra and Oehrlein [18] have used the STM to observe the effect of low energy argon-ion bombardment on the morphology of Si(100). The Si(111)-2×1 reconstruction was studied [19] confirming the π-bonded chain model. The surfaces of GaAs [20] and Ge [21] have also been investigated.

Fig. 3 shows STM results [22] for the Au(100) surface with single atom high steps and large areas that are atomically flat. The 1×5 reconstruction can be seen directly. Other studies of metal substrates include the effect of steps on the chemisorption system of oxygen on Ni(110) [23] and on the boundaries of rotational domains on reconstructed Pt(100) [24], and the morphology of deposited Ag films [25].

The STM has been applied to samples under a wide variety of conditions. It has been used at low temperatures to study [26] the electronic structure of superconducting Nb_3Sn and to image [27] charge density waves on 1T-TaS_2. It has been used with air [28,29], water [30], and liquid nitrogen [27] in the tunneling gap. It is also being used in technical applications to extend the conventional ways the surface roughness of manufactured parts is measured [31,33]. It is being investigated as a means of extending our ability to do lithography [34,35]. And finally, its possible application to biological systems is being investigated [36].

New types of STM are constantly being introduced. One significant advance is the ability to scan at high speeds [37]. Another modification is the use [13] of an STM in conjunction with a scanning electron microscope. Perhaps

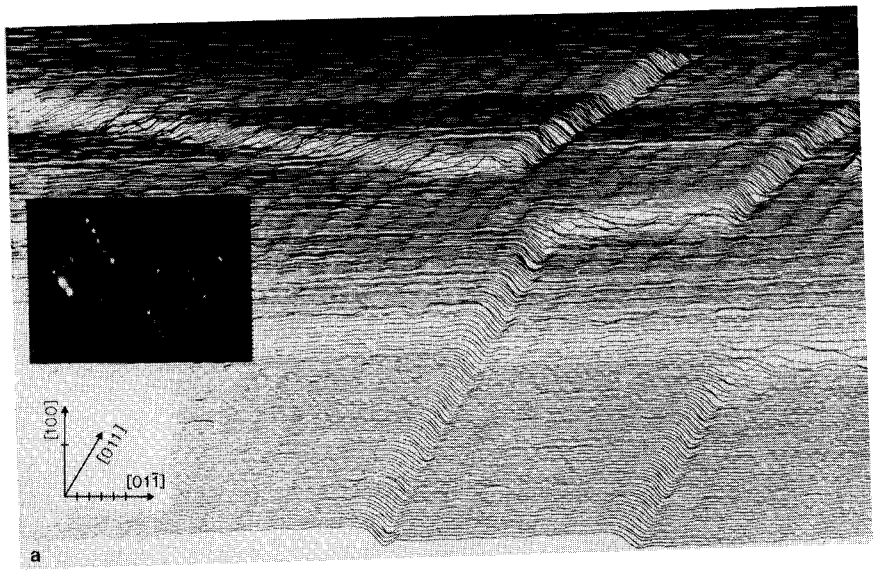

Fig. 3. STM picture of the 1×5 reconstruction of the Au(100) surface showing "flat" regions separated by monoatomic steps. A LEED photo of the reconstruction is superimposed. Taken from ref. [22].

the most far reaching change is the extension of the technique to include systematic variation of the gap bias voltage. This method is referred to as current imaging tunneling spectroscopy (CITS) [38]. Here the servo system is momentarily turned off at each point above the surface and a tunnel current versus gap voltage curve is taken before the tip drifts out of position. The resulting measurement consists of perhaps 50 images of the same surface region, each taken from the same distance but at a different gap voltage. Since a modification of the gap potential changes the filled and empty states that contribute to the tunneling current, it is possible to spatially resolve both types of states. Recent work by Hamers et al. [38] has resolved both the filled and empty surface states of the Si(111)-7×7 reconstruction with 3 Å resolution. The use of this spectroscopy will extend the use of the STM from a tool to study surface physical structure to one which can, in addition, study spatially resolved electronic structure.

3. Scanning electron microscopy with polarization analysis

Microscopic magnetic phenomena can be very important and are studied for many of the same reasons that physical microstructures are. Size effects

and the two-dimensional nature of single-atom layers give rise to interesting and difficult to predict magnetic domain structures. The physical microstructure can have a significant effect on the magnetic microstructure and, consequently, on the magnetic properties of the material. The desire for high density magnetic recording devices and media also contribute to the current interest in bettering our understanding of magnetic microstructure, as does our ability to fabricate new layered magnetic materials using the techniques of molecular beam epitaxy.

Domain observations have been made by a number of techniques [39]. The Bitter method utilizes a fine magnetic powder applied to the surface which responds to the stray magnetic field by collecting at the points of high field gradients, e.g. domain walls. The Kerr effect is an example of a magneto-optical interaction in which the polarization of incident radiation is modified by the effect the magnetization has on the optical constants of the sample. Both of these techniques employ optical observation of the patterns which limits the resolution which can be obtained to about 1 μm. Domain observation in an electron microscope is achieved because an electron moving within the sample will be slightly deflected by a magnetic field normal to the direction of motion. Transmission electron microscopy of appropriately thinned samples allows imaging of domains below the optical resolution limit. The magnetic contrast in the image reflects the value of the line integral of the transverse magnetic field through the sample thickness.

A new method for domain imaging [40], scanning electron microscopy with polarization analysis (SEMPA), permits the measurement of the *vector* magnetization of the volume of a surface lying under the incident electron beam of a scanning electron microscope. The new technique was suggested by an experiment [41] which analyzed the intensity and polarization distributions of secondary electrons ejected from a ferromagnetic sample by an incident unpolarized electron beam. The spin polarization of the ejected electrons was found to reflect, both in magnitude and direction, the magnetization of the surface volume lying under the incident electron beam.

3.1. Method

Magnetism in a ferromagnet derives from a preferential alignment of spin magnetic moments in some direction. If these electrons are ejected from the solid without any significant change in spin direction, then a measurement of the spin orientation of the ejected electrons will provide both the direction and magnitude of the magnetization. Such electron beam polarization measurements can be accomplished by a variety of techniques [42]. One measures the electron spin polarization along a given direction, for example, $P_z = (N_\uparrow - N_\downarrow)/(N_\uparrow + N_\downarrow)$, where $N_\uparrow$ and $N_\downarrow$ are respectively the number of electrons in the beam with spins parallel and antiparallel to the $+z$ direction. Generali-

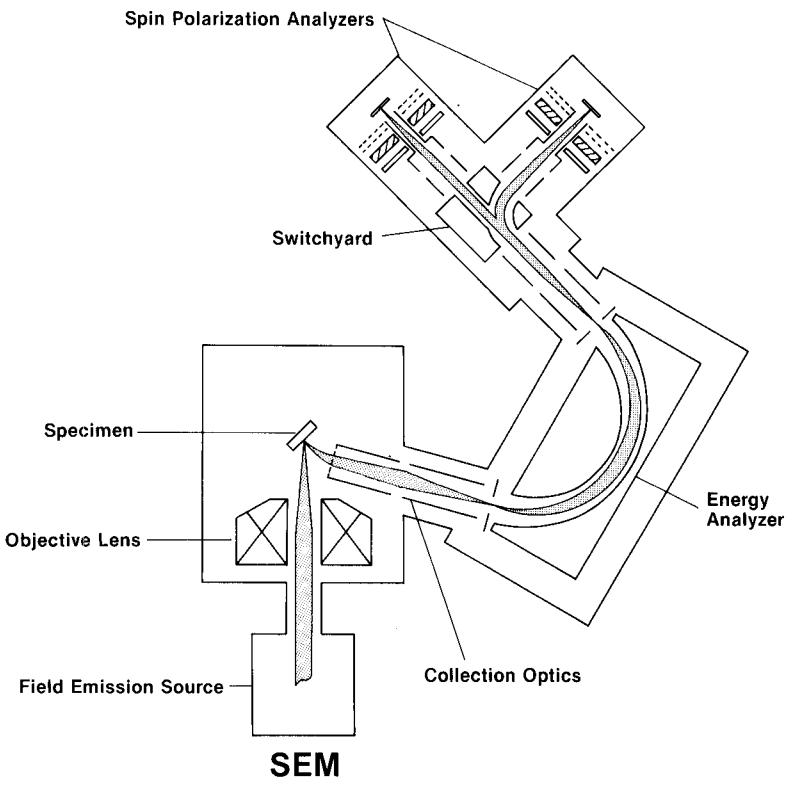

Fig. 4. Schematic view of the scanning electron microscope with two orthogonal polarization detectors to measure all three components of the electron spin polarization. The detectors and the optional energy analyzer are shown much larger than full scale for clarity. Taken from ref. [43].

zation to the measurement of all three cartesian polarization components is straightforward.

A conventional scanning electron microscope produces a topographic image of a surface by rastering a highly focused incident electron beam across a sample, collecting the ejected low energy secondary electrons, and intensifying a synchronously rastered display in proportion to the number of secondaries ejected from each position on the sample. If polarization detection is added to the microscope [43], as shown schematically in fig. 4, the secondary electrons may be additionally interrogated to reveal the sample magnetization. It is an important feature of this technique that the magnetization information provided by a measurement of the electron polarization is independent of the topographic information conveyed by the simultaneous measurement of the number of secondary electrons. The intrinsic spin of the electron provides an

additional information channel that has not previously been utilized.

Since the secondary electrons detected originate in the near-surface region, SEMPA measurements are intrinsically surface sensitive. Consequently, the UHV environment of either a scanning Auger microprobe or a UHV scanning electron microscope is required. While an important advantage of the SEMPA technique is that very thin samples are not necessary, the technique is also not degraded when thin film samples are investigated.

The choice of polarization detector is important. At NBS, a detector has been especially designed for SEMPA measurements [44]. Its salient features include operation at a reasonable energy (150 eV), small size, high efficiency, and the acceptance of electron beams with the broad energy distribution characteristic of secondaries. Other detector choices, though not without disadvantages, include the high energy (120 keV) Mott detector [42] or the LEED detector [42,45].

3.3. *Applications of SEMPA*

SEMPA is in its infancy as an experimental technique. At the time of this writing only two laboratories have completed the adaptation of an instrument for SEMPA measurements. The first images were produced using a high energy Mott detector and a UHV sample chamber to which a scanning electron gun with a beam diameter of 10 μm was attached [46]. In initial studies [46,47] domains of Fe(001) and Co($1\bar{2}10$) surfaces were imaged. The electron gun was subsequently improved to obtain a spatial resolution of 100 nm [48,49].

In the approach illustrated in fig. 4 a commercial UHV scanning electron microscope with a field emission source was employed. The brightness of the field emission gun permits probe sizes down to of order 10 nm. Also, multiple orthogonal detectors are used to allow determination of all three components of the electron polarization. The energy selector shown is optional for this purpose and is present to allow for the use of spin polarized Auger spectroscopy [50]. This apparatus has been used [43,51–52] to image a variety of magnetic systems and devices. An example of a polarization image for Fe(001) is shown in fig. 5b along with the accompanying intensity image in fig. 5a. The surface was cleaned by ion sputtering and then annealed. The intensity image is typical of that of a polished surface. Scattered defects and scratches are visible with a prominent defect positioned centrally. The polarization image in fig. 5a exhibits four distinct levels of gray shading which signal four distinct values for the component of polarization in the x-direction. This is to be expected because they correspond to the four anisotropy directions of the cubic lattice of the Fe crystal. The arrows indicate the orientations of the local magnetization, which are typical of the closure domains found on this crystal face. The explanation of the zig-zag pattern of the domain wall between

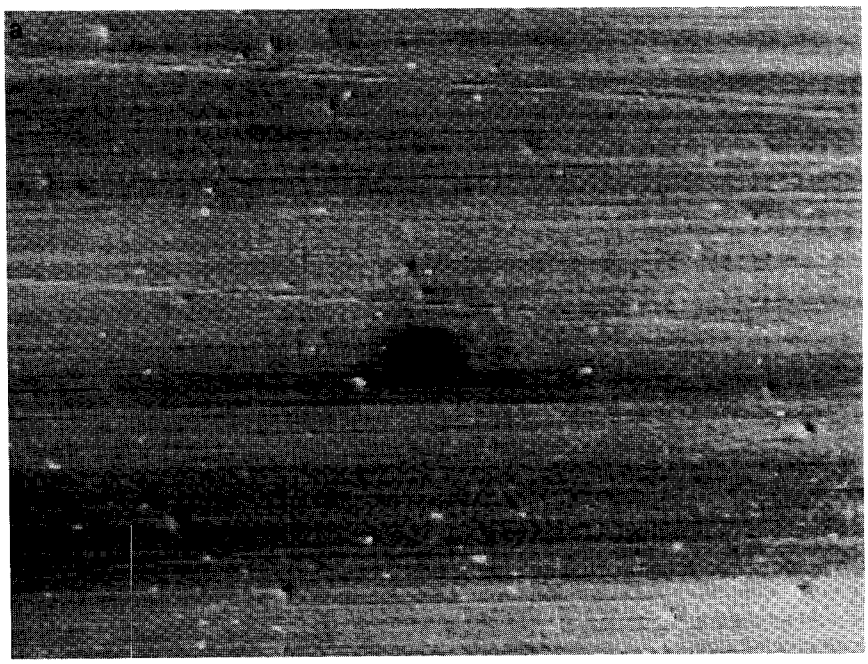
a


b

Fig. 5. (a) A conventional SEM micrograph of a Fe–3%Si polished crystal surface with an x-axis length of 100 μm. (b) The simultaneously obtained map of the domain structure of the same region. This crystal is expected to exhibit four in-plane easy axes of magnetization because of the cubic lattice anisotropy. The four shades of gray indicate the four possible domain orientations as indicated by the arrows. The domains are unaffected by most of the small surface defects, but are modified by the large defect at the center of the image.

regions of opposing magnetization seen in the upper right corner has been discussed previously [53].

Many new applications of the SEMPA technique are being pursued. In contrast to the other electron microscope techniques used, the magnetization image does not depend on the surface topography except as the topography affects the magnetic structure. SEMPA studies of the effect of physical structure on magnetic structure therefore hold great promise. Examples include the source of the high coercivity in NdFeB magnets, the modification of domain structure as the size and thickness of permalloy structures are varied, and research into structure induced anisotropies in CoCr recording media. High resolution studies of the spin structure within domain walls are to be expected. High resolution scanning Auger microprobe systems, incorporating the SEMPA technique, will allow the further correlation of magnetic structure with chemical composition. Finally, these microscopic measurements should extend and complement the other very active areas of polarized electron research [52], e.g. photoemission, inverse photoemission, and electron scattering.

Acknowledgements

I wish to acknowledge the helpful suggestions of my colleagues D.T. Pierce and J. Unguris. This work was supported in parts by the Office of Naval Research.

References

[1] See also the IBM Journal of Research, July and September 1986.
[2] D.J. Whitehouse, Stylus Techniques, in: Characterization of Solid Surfaces, Eds. P.F. Kane and G.B. Larrabee (Plenum, New York, 1974) ch. 3.
[3] R.D. Young, J. Ward and F. Scire, Rev. Sci. Instr. 43 (1972) 999.
[4] R.D. Young, Phys. Today 24 (1971) 42.
[5] R.D. Young, J. Ward and F. Scire, Phys. Rev. Letters 27 (1971) 922.
[6] E.C. Teague, PhD Thesis, North Texas State University, Denton, TX (1978).
[7] G. Binnig, H. Rohrer, Ch. Gerber and E. Weibel, Phys. Rev. Letters 50 (1982) 120.

[8] J. Bardeen, Phys. Rev. Letters 6 (1961) 57.
[9] J. Tersoff and D.R. Hamann, Phys. Rev. Letters 50 (1983) 1998.
[10] J. Tersoff and D.R. Hamann, Phys. Rev. B31 (1985) 805.
[11] G. Binnig and H. Rohrer, Helv. Phys. Acta 55 (1982) 726.
[12] G.F.A. van de Walle, J.W. Gerritsen, H. van Kempen and P. Wyder, Rev. Sci. Instr. 56 (1985) 1573.
[13] Ch. Gerber, G. Binnig, H. Fuchs, O. Marti and H.J. Rohrer, Rev. Sci. Instr. 57 (1986) 221.
[14] J.E. Demuth, R.J. Hamers, R.M. Tromp and M.E. Welland, IBM J. Res. Develop. 30 (1986) 396.
[15] R.S. Becker, J.A. Golovchenko, D.R. Hamann and B.S. Swartzentruber, Phys. Rev. Letters 55 (1985) 2032.
[16] R.S. Becker, J.A. Golovchenko, E.G. McRae and B.S. Swartzentruber, Phys. Rev. Letters 55 (1985) 2028.
[17] G. Binnig, H. Rohrer, F. Salvan, Ch. Gerber and A. Baro, Surface Sci. 157 (1985) L373.
[18] R.M. Feenstra and G.S. Oehrlein, Appl. Phys. Letters 47 (1985) 97.
[19] R.M. Feenstra, W.A. Thompson and A.P. Fein, Phys. Rev. Letters 56 (1986) 608.
[20] R.M. Feenstra and A.P. Fein, Phys. Rev. B32 (1985) 1394.
[21] R.S. Becker, J.A. Golovchenko and B.S. Swartzentruber, Phys. Rev. Letters 54 (1985) 2678.
[22] G. Binnig, H. Rohrer, Ch. Gerber and E. Stoll, Surface Sci. 144 (1984) 321.
[23] A.M. Baro, G. Binnig, H. Rohrer, Ch. Gerber, E. Stoll, A. Baratoff and F. Salvan, Phys. Rev. Letters 52 (1984) 1304.
[24] R.J. Behm, W. Hosler, E. Ritter and G. Binnig, Phys. Rev. Letters 56 (1986) 228.
[25] J.K. Gimzeewski, A. Humbert, J.G. Bednorz and B. Reihl, Phys. Rev. Letters 55 (1985) 951.
[26] S.A. Elrod, A.L. Lozanne and C.F. Quate, Appl. Phys. Letters 45 (1984) 1240.
[27] R.V. Coleman, B. Drake, P.K. Hansma and G. Slough, Phys. Rev. Letters 55 (1985) 394.
[28] Sang-li Park and C.F. Quate, Appl. Phys. Letters 48 (1986) 112.
[29] B. Drake, R. Sonnenfeld, J. Schneir, P.K. Hansma, G. Slough and R.V. Coleman, Rev. Sci. Instr. 57 (1986) 441.
[30] R. Sonnenfeld and P.K. Hansma, Science 232 (1986) 211.
[31] N. García, A.M. Baro, R. Miranda, H. Rohrer, Ch. Gerber, R.G. Cantu and J.L. Peña, Metrologia 21 (1985) 135.
[32] R. Miranda, N. García, A.M. Baro, R. García, J.L. Peña and H. Rohrer, Appl. Phys. Letters 47 (1985) 367.
[33] R.A. Dragoset, R.D. Young, H.P. Layer, S.R. Mielczarek, E.C. Teague and R.J. Celotta, Opt. Letters 11 (1986) 560.
[34] M. Ringger, H.R. Hidber, R. Schlogl, P. Oelhafen and H.-J. Guntherodt, Appl. Phys. Letters 46 (1985) 832.
[35] M.A. McCord and R.F.W. Pease, J. Vacuum Sci. Technol. B4 (1986) 86.
[36] A.M. Baro, R. Miranda, J. Alaman, N. García, G. Binnig, H. Rohrer, Ch. Gerber and J.L. Carrascosa, Nature 315 (1985) 253.
[37] A. Bryant, D.P.E. Smith and Q.F. Quate, Appl. Phys. Letters 48 (1986) 832.
[38] R.J. Hamers, R.M. Tromp and J. Demuth, Phys. Rev. Letters 56 (198) 1972.
[39] D.J. Craik, in: Methods of Experimental Physics, Vol. 11, Ed. R.V. Coleman (Academic Press, New York, 1974) pp. 675–743.
[40] A.L. Robinson, Science 230 (1985) 53.
[41] J. Unguris, D.T. Pierce, A. Galejs and R.J. Celotta, Phys. Rev. Letters 49 (1982) 72.
[42] J. Kessler, Polarized Electrons (Springer, Berlin, 1985).
[43] J. Unguris, G.G. Hembree, R.J. Celotta and D.T. Pierce, J. Magnetism Magnetic Mater. 54/57 (1986) 1629.
[44] J. Unguris, D.T. Pierce and R.J. Celotta, Rev. Sci. Instr. 57 (1986) 1314.
[45] J. Kirschner, Polarized Electrons at Surfaces (Springer, Berlin, 1985).

[46] K. Koike and K. Hayakawa, Japan. J. Appl. Phys. 23 (1984) L187.
[47] K. Koike and K. Hayakawa, Appl. Phys. Letters 45 (1984) 585.
[48] K. Koike and K. Hayakawa, J. Appl. Phys. 57 (1985) 4244.
[49] K. Koike, H. Matsuyama, H. Todokoro and K. Hayakawa, Japan. J. Appl. Phys. 24 (1985) 1078.
[50] M. Landolt, in: Polarized Electrons in Surface Physics, Ed. R. Feder (World Scientific, Singapore, 1985).
[51] J. Unguris, G.G. Hembree, R.J. Celotta and D.T. Pierce, J. Microscopy 139 (1985) RP1.
[52] R.J. Celotta and D.T. Pierce, Science 234 (1986) 333.
[53] S. Chikazumi and K. Suzuki, J. Phys. Soc. Japan 10 (1955) 523.